



On the use of Fire Safety Engineering to Evaluate the Performance of Heat Detectors in High Ceiling Application

Mattia Carboni ^a, Lorenzo Rossi ^b, Paolo Mocellin ^{a,*}

^a Dipartimento di Ingegneria Industriale, Università degli Studi di Padova. Via Marzolo 9, 35131 Padova, Italia.

^b SPR Tecnologie Srl, Via Niccolò Machiavelli 1/b, Zola Predosa, 40069, Bologna, Italia.

In the framework of design and installation of fire detection and fire alarm system in buildings, when high ceilings are involved, it is likely to run into the limits of the more common standards. Several regulations fix a ceiling height limit beyond which heat, smoke, and combustion gas detectors should not be mounted. Among the available technologies, the aspirating smoke detection (ASD) systems have the highest limit (i.e., 40 m according to BS 5839-1:2017). Nevertheless, this technology should not be used when processes that yield smoke, fumes, dust, etc., are present, and an alternative type of fire detector needs to be employed. This is due to the necessity to avoid false alarms, which is critical for successful fire detection and alarm systems. The concomitance of these two situations, i.e., dusty environments and high ceiling height, is not unusual in the industrial sectors. To investigate it, the state-of-the-art solution is adopting the principles of Fire Safety Engineering (FSE). The FSE is based on calculations that consider the conservation of mass and energy and permit to predict several crucial quantities such as the smoke temperature, smoke volume (and layer height), and species concentrations resulting from a fire of a given size (ISO/TS 13447:2013). In this work, a series of Computational Fluid Dynamics (CFD) simulations were conducted to assess the performances of a fire detection system composed of heat detectors installed at heights up to 20 m larger than the standard limit. The characteristics of an actual building adopted for storage of hazardous materials and a real heat detector system were considered. The temperature field resulting from two different types of t^2 -growth fire, i.e., one ultra-fast and one with slow evolution, were analyzed. The corresponding alarm times were evaluated and compared with ASD characteristics timings, recognized as a benchmark for its high sensitivity.

1. Introduction

Fire detectors are designed to detect at least one of the four characteristics of fire: heat, smoke, carbon monoxide, and infrared or ultraviolet radiations (BSI, 2017). The technology chosen should provide adequate protection of occupants minimizing false alarms. At this aim, it is essential to individuate the kind of fire expected and the characteristics of the environment in which the system should be installed. For example, heat detectors may not be installed in areas in which products of combustions might be corrosive and consequently can cause considerable damage without burning the contents of the affected area. On the other hand, smoke detectors should not be used when the principal fire hazard is the presence of flammable liquids or gases that produce little smoke or in areas in which smoke detectors would have a high potential for false alarms. Moreover, flame detectors should only be used in situations in which it is sufficient for the fire detection system to respond to flaming fires, but not fires that produce smoke without significant flames (e.g., smouldering fires). In contrast, ultraviolet flame detectors should not be used as the sole means of fire detection in areas within buildings in which a fire can produce significant quantities of smoke before flaming occurs. In addition to standard technologies, more sophisticated solutions have been developed. For example, the aspirating smoke detection systems (ASD) can also guarantee a very high sensitivity to detect smoke that has been substantially diluted with clean air. On the heat side, a more efficient way to detect a fire is to analyze the pressure variation inside a tube filled with air installed in the monitoring area. An example of this system is the one developed by Securiton, named Securisens ADW (Securiton, 2021). More details can be retrieved in the following chapters. In Table 1, the abovementioned characteristics are resumed and compared for a monitoring area of 2500 m². Moreover, the ceiling limits refer to BSI 5839-1:2017 (BSI, 2017). For the heat detectors, 9.0 m is referred to as

Class A1 system, while the values of 40 m is for Class B ASD system with at least 15 holes or for optical beam with enhanced sensitivity (alarm at 35% attenuation or less).

Table 1: Comparison of the most common fire detection system technologies.

Technology	Economic affordability		Types of revelation		Environment			Ceiling Height [m]	False Alarm Resistance
	Installation	Maintenance	Very Clean Fires	Smouldering Fires	Open	Closed	Dusty		
Securisens ADW	€€€€	€€	+++++	+	+++++	++++	+++++	7.5/9.0	+++++
Point heat detectors	€€€€	€€€€€	+++	++	++	+	++++	7.5/9.0	+++
ASD	€€€	€€€	+++	+++++	++	+++++	+	40.0	++
Point smoke detectors	€€€	€€€€€	++	+++	+	+++	++	10.5	+++
Optical Beam	€€	€€€€	+	++	+	++	++	40.0	+

Quite clearly, one of the main parameters to consider is the ceiling height limit. Based on BSI 5839-1:2017 (BSI, 2017), when ceilings higher than 10.5 m are present, only the optical beam and the ASD can be employed. Indeed, optical beam detectors and aspirating smoke detection systems are less sensitive to the effects of ceiling height since the increased size of the plume will involve a more significant proportion of the path length of the optical beam or more sampling holes, alleviating the effects of reduced smoke density. Nevertheless, these technologies should not be used when processes that yield smoke, fumes, dust, etc., are present (i.e., dusty environments), which are not rare conditions in the industrial field (Vianello et al., 2020; Mocellin and Maschio, 2016).

In this work, the performances of the Securisens ADW detection system (i.e., a linear heat detector) in a building adopted for storage of hazardous materials with a height larger than the one recommended by BSI 5839-1:2017 (BSI, 2017) were evaluated through computational fluids dynamics (CFD) (Vianello et al., 2014). Results are analyzed in terms of alarm times, temperature fields, and radiative heat fluxes.

2. Materials and method

The software employed in this work is Fire Dynamics Simulator (FDS), which is a computational fluid dynamics (CFD) model of fire-driven fluid flow. FDS solves numerically a form of the Navier-Stokes equations appropriate for low-speed ($Ma < 0.3$), thermally-driven flow, emphasizing smoke and heat transport from fires (Mocellin et al., 2021). The formulation of the equations and the numerical algorithm are contained in the FDS Technical Reference Guide. In addition, some verified and validated models are discussed in the Verification (McGrattan et al., 2013) and Validation (McGrattan et al., 2019b) guides. This software has already been employed either to evaluate the performances of ASD systems (Huang et al., 2020) (He and Jiang, 2005) or for heat detectors (Hurley and Munguia, 2007). In the following sections, the characteristics of the building and the alarm system considered are reported together with the design fire scenarios and the geometrical domain.

2.1 Building geometrical characteristics

The considered building is designed for the storage of hydrocarbons waste. The geometrical structure was simplified for the CFD simulations as in Figure 1a. More specifically, the building is formed by a single volume with a base of 43.8 m (x-direction) x 44.4 m (y-direction). The ceiling height of the structure is 13.0 m in the central part (h_{max}) and 10.3 m in the lateral ones (h_{min}). The central part is 20.5 m wide (x-direction). Two doors of $(6 \times 5) \text{ m}^2$ and 11 vents of $(1.7 \times 1.8) \text{ m}^2$ and 13 rectangular storage bays are present. The storage bay boundary walls are 6.0 m high from the floor (z-direction) and 13.3 m long (x-direction). On the other hand, in the y-direction, the lengths vary from 4.60 m to 6.20 m. The bays were uniquely identified and numbered, as shown in Figure 1b. The red bays were selected for the fire scenarios (more details are reported in the following chapter). Considering the construction materials, all the components, except the fuel matrices, were assumed as inert.

2.2 Fire scenarios

Two design fire scenarios were identified to evaluate the response of the alarm system in case of slow and rapid (i.e., ultra-fast) fires. Both considered a pre-flashover condition, but the first is of interest for the system response in terms of early detection, while the second is for the individuation of the possible radiative heat flux (q). Two possible fire positions were considered: one originated from Bay No. 1 (60 m^2) and one from Bay No. 9 (68 m^2). In both cases, the bays were considered half-filled (i.e., filled up until a height of 3.0 m from the floor). Bay No. 1 was considered significant for the angular position in the domain, close to a ventilation opening, while Bay No.

9, because of the central position and proximity to the ventilation opening generally also used as access to the area. The other combustion parameters employed were retrieved from the Italian fire safety regulations dealing with FSE (VVF, 2021) and reported in Table 1. Furthermore, the initial ambient temperature (T_a) was set equal to 20°C for all tests. Starting from these considerations, four simulations were conducted (Table 1).

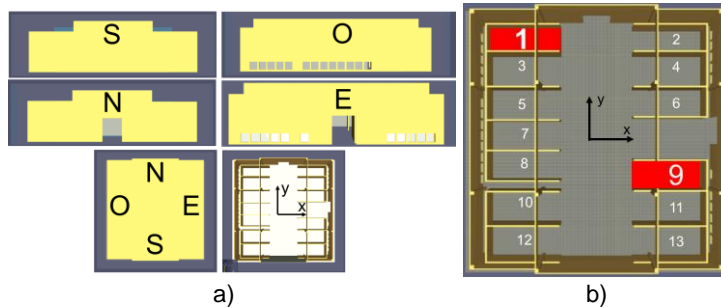


Figure 1: Geometrical characteristics of the building considered.

Table 1: Main input parameters of the four simulations conducted.

Parameter	TEST1	TEST2	TEST3	TEST4
Fire growth rate [s]	600 (slow)	600 (slow)	75 (ultra-fast)	75 (ultra-fast)
Heat Release Rate per Area (HRRPUA) [kW m ⁻²]	500	500	1000	1000
Position, bay [#]	1	9	1	9
Heat of combustion [MJ kg ⁻¹]	20	20	20	20
CO yield (y_{CO}) [kg/kg]	0.1	0.1	0.1	0.1
Soot yield (y_{soot}) [kg/kg]	0.18	0.18	0.18	0.18
Hydrogen fraction [-]	0.10	0.10	0.10	0.10
Radiative fraction [-]	0.35	0.35	0.35	0.35

2.3 Numerical domain

The numerical domain was set to 50 m (x-direction, length), 50 m (y-direction, height), and 40 m (z-direction, wide), and a structured grid with cubic cells employed. The selection of proper cell sizes (δ) was made under the grid resolution criterion suggested in the literature (McGrattan et al., 2019a). More specifically, the characteristic diameter (D^*) to δ ratio was kept at 12 and 13 in the cases of slow and ultrafast fires respectively, to guarantee a medium meshes and an affordable computational time. Indeed, the FDS User Guide (United States Nuclear Regulatory Commission, 2007) has defined a $D^* \delta^{-1}$ below 10 representatives for coarse mesh, between 10 and 16 as per medium mesh, and larger than 16 as per fine mesh. In addition to that, a sensitivity analysis was conducted. More details are discussed in the chapter of results.

2.4 Alarm system

The detection alarm system employed is the Securisens ADW developed by Securiton (Securiton, 2021). It is a linear heat detector consisting of a capillary tube filled with air installed in the area to be monitored. A pressure sensor constantly analyzes the pressure inside the tube, and the processing electronics compare the detected value with the alarm criteria. This system is EN 54-22 approved (BSI, 2013) and is typically installed in tunnels, underground garages, food and chemical industry, waste processing plants, high-temperature applications, etc. For the implementation in the software, it has been assimilated to a set of heat detectors positioned following the reference standard (UNI, 2013). Considering the monitoring area of the present work, the Securiton software tool ADW-HeatCalc reports a Class A1 behaviour (BSI, 2013). For the description of the dynamics of the sensors, it was considered the following equation (Equation 1) (McGrattan et al., 2019a):

$$\frac{dT_r}{dt} = \frac{\sqrt{|u|}}{RTI} (T_g - T_r) \quad (1)$$

where T_r is the detector temperature (°C), u is the gas velocity (m s⁻¹) and T_g is the gas temperature (°C). RTI or response time index is expressed in m^{1/2}s^{1/2} and represents a measure of the sensitivity of the detection system referred to as NFPA 72 (NFPA, 2019). The lower the RTI, the more sensitive is the unit in the fire detection process (Schifiliti, 2006), and indeed, the RTI can be used to determine how a device responds to a given fire scenario. Since the ADW 535 is approved by FM Global's independent testing laboratory according to FM 3210 (NFPA, 2018) and tested as an open space detector with spacing from 4.5 m to 12 m (NFPA, 2019), it is possible to use the tables in Annex B of FM 3210 (NFPA, 2018) as a guide for RTI. Therefore, if the ADW

appliance is installed considering a spacing $(9 \times 9) \text{ m}^2$ (UNI, 2013) and a temperature rating (T_r) of 71°C , it is possible to state that the RTI will be lower than $275 \text{ m}^{1/2}\text{s}^{1/2}$. Concerning the aforementioned temperature rating, to reduce the probability of false alarms, it must be at least 11°C higher than the maximum expected ambient temperature (Schifiliti, 2006). The detection system, consisting of a network of detectors, was positioned as shown in Figure 2, following the abovementioned spacing. The detectors were considered installed 0.20 m lower than the ceiling.

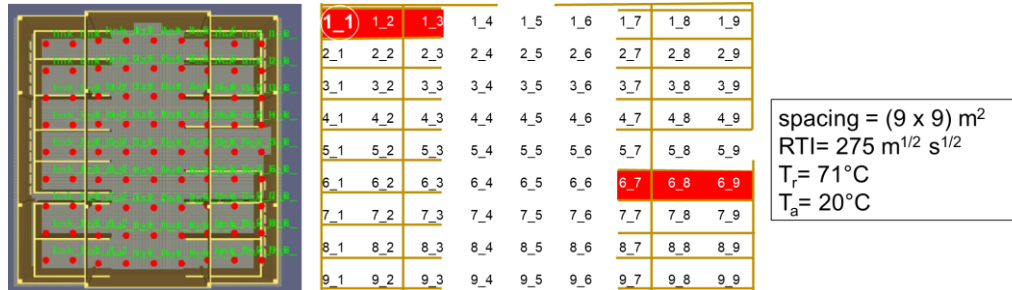


Figure 2: Positioning, nomenclature, and main parameters of the heat detectors employed.

3. Results and discussion

As previously mentioned, a sensitivity analysis was conducted. More specifically, it was analyzed the temperature registered by sensor 1_1 in the case of TEST 1, and the maximum percentage variation (Δ_{i-fine}) between the analyzed (i.e., i) and the most refined (i.e., fine) mesh considered as monitoring parameter.

Table 3: Results of the sensitivity analysis conducted.

Mesh type	δ [m]	$D^* \delta^{-1}$	Δ_{i-i} [%]
Coarse	1.000	3	19
Coarse	0.500	6	9
Medium	0.250	12	6
Fine	0.125	23	-

The maximum percentage variation equal to 6% registered in the case of medium mesh was retained acceptable for the quantities analyzed in this study. For this reason, a cell size (δ) equal to 0.250 m was adopted for all the tests. In the following, the main results of the simulations described are reported. More specifically, the time at which the fire detection system is alarmed (t_{alarm}) with the respective temperature field and radiative heat fluxes (q) are described. Moreover, the dependence of the t_{alarm} on the ceiling height is analyzed.

3.1 Fire detection efficiency

Firstly, the times at which the first three sensors in the four simulations were activated are reported in Table 3.

Table 3: Time for alarm (t_{alarm}) and number identification of the first three sensors activated.

$t_{alarm,i}$ (sensor #)	TEST1	TEST2	TEST3	TEST4
$t_{alarm,1}$	174 s (1_1)	160 s (7_9)	38 s (1_1)	36 s (7_9)
$t_{alarm,2}$	188 s (2_1)	174 s (6_9)	40 s (2_1)	38 s (6_9)
$t_{alarm,3}$	206 s (1_2)	178 s (8_9)	44 s (1_2)	40 s (6_8)

Quite obviously, the more considerable times were obtained for TEST1 (174 s) and TEST2 (160 s), with slow-growth fire scenarios. On the other hand, for the ultra-fast scenario, the system is activated in less than 40 s. Considering the position of the fires, Bay. No. 9 produces lower alarm times, probably due to the larger area. No particular differences were retrieved in the position of the activated sensors. Indeed, only sensors 8_9 (TEST 2) and 6_8 (TEST 4) differ for $t_{alarm,3}$. Nevertheless, for TEST 2, sensor 6_8 is activated only 10s after sensor 8_9. In addition to that, the main result that can be retrieved from Table 2 is that based on these simulations, the system seems to be effective in detecting the fire despite the out of standards ceiling height. Indeed, to compare the alarm times, the UNI/TR 11694:2017 directive (UNI, 2017) was taken into account. Here, field tests that simulate a fire principle are recommended to verify the correct functioning of ASD systems, recognized as very high sensitivity (BSI, 2017). For heights greater than 3 m , it is recommended to use smoke tabs. In this case, the system shall detect a response within 180s since the burner is switched off. In the simulations performed, this time is respected even in the worst case (174s).

3.2 Heat fluxes and temperature fields

In this section, the temperature field at t_{alarm} retrieved in TEST1 is reported (Figure 3). For the sake of brevity, the other tests are not shown. On the other hand, the radiative heat fluxes at the alarm time ($q_{t_{alarm}}$) are reported for all the tests (Table 4).

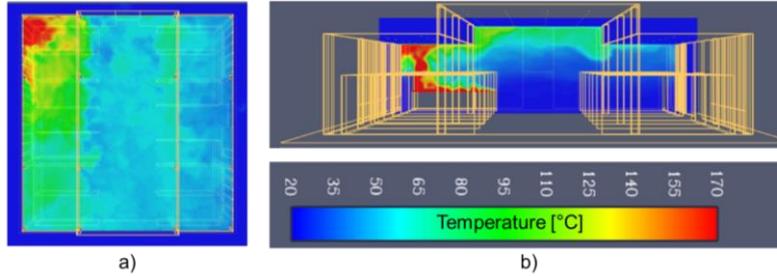


Figure 3: Temperature field at the alarm times in the vertical (a) and cross at the height of the detection system (b) sections.

Table 4: Radiative heat flux at alarm time ($q_{t_{alarm,i}}$) expressed in kW m^{-2} of the first three sensors activated.

$q_{t_{alarm,i}}$ [kW m^{-2}] (sensor #)	TEST1	TEST2	TEST3	TEST4
$q_{t_{alarm,1}}$	8.68 (1_1)	4.46 (7_9)	22.30 (1_1)	17.38 (7_9)
$q_{t_{alarm,2}}$	2.22 (2_1)	5.57 (6_9)	11.03 (2_1)	50.25 (6_9)
$q_{t_{alarm,3}}$	13.50 (1_2)	0.86 (8_9)	23.71 (1_2)	16.64 (6_8)

The temperature fields obtained in the two tests have a slightly different scale. As a matter of fact, the maximum temperature registered in TEST1 is 170°C , while in TEST4, characterized by ultra-fast fire growth rate and higher HRRPUA, is 570°C . Moreover, it is possible to observe from the cross-sections (Figure 3b and Figure 3d) that the fire developed preferentially in the direction of the boundary walls rather than the central part. This suggests putting an increased number of devices in this area to enhance the performance of the system with respect to the standard design. A similar result is obtained for the heat fluxes, for which a maximum value of 50.25 kW m^{-2} is obtained for TEST4 compared to the maximum value of 13.50 kW m^{-2} of the tests with lower HRRPUA (i.e., TEST1 and TEST2). These values could be helpful for structural evaluation.

3.3 Alarm time as a function of ceiling heights

In order to explore the possibility to employ the proposed system also at higher ceiling heights, other 3 simulations, with the same features of TEST1 (i.e., the one with the slower alarm time), except for the ceiling heights, were conducted. More specifically, the ceiling heights (h_{min} and h_{max}) were firstly doubled (20.6 m and 26 m) and then tripled (30.9 m and 39 m). Moreover, a simulation was conducted at the highest limit of the BSI 5839-1:2017 (i.e., 9.0 m) (BSI, 2017) (6.1 and 9.0 m). The t_{alarm} were then plotted as a function of h_{min} (Figure 4a), and the sensors which were resulted activated at time equal to 400s (i.e., the time necessary to appreciate also the results of the highest ceiling case) were highlighted in Figure 4b, Figure 4c, and Figure 4d.

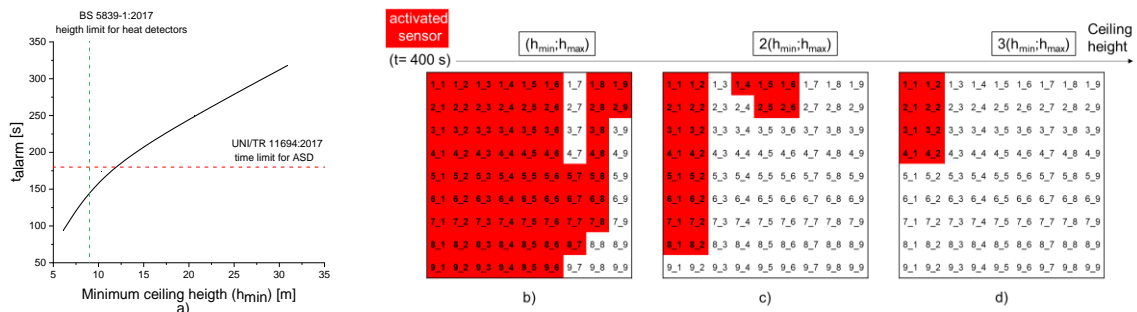


Figure 4: a) t_{alarm} as a function of the minimum ceiling height (h_{min}). Sensors activated in a time of 400 s in the case of TEST1 (b), TEST1 with a $2h_{min}$ (c) and TEST1 with a $3h_{min}$ (d).

As it is possible to see from Figure 4a, the reported trend could be approximated by Equation 2 ($R^2 = 0.994$):

$$t_{alarm}(h_{min}) = 134 \cdot \ln(h_{min}) - 145 \quad (2)$$

Based on the results of these simulations, in order to respect the time limit of the UNI/TR 11694:2017 Directive (UNI, 2017), a maximum h_{min} of 11.5 m is allowed. After this value, a delay on the 180 s of about 10 s per m has to take into consideration. Furthermore, when the ceiling height is increased, an even smaller number of sensors reveal the fire. Indeed, 400s from the start of fire growth, 83% of sensors are alarmed at h_{min} , while at $2h_{min}$ the 26%, and at $3h_{min}$ only 10% of sensors. This confirms the decrease in efficiency as the height increases.

4. Conclusions

In this work, a series of CFD simulations were conducted to assess the performances of heat detectors installed at non-standard elevation values in an industrial building in which a dusty environment does not allow smoke detection-based technologies, which are more effective at high-ceiling heights. Based on these simulations, a good response of the system was reported until the height of 11.5 m (height of revelation). However, a relevant decline in the efficacy of the arrangement in terms of response time delay and numbers of alarmed sensors were retrieved beyond this value. In addition, temperature field results suggest considering an increased number of sensors in the perimeter area in the design stage, where the fire seems to propagate preferentially.

Acknowledgments

The authors acknowledge the contribution of Mr. Dennis Giusti and Mr. Marco Roversi (SPR Tecnologie).

References

- BSI, 2017. BSI 5839-1:2017, Fire detection and fire alarm systems for buildings. BSI Stand. Publ.
- BSI, 2013. BS EN 54-22:2015+A1:2020 BSI, Fire detection and fire alarm systems. BSI Stand. Publ.
- He, M., Jiang, Y., 2005. Use FDS to Assess Effectiveness of Air Sampling-Type Detector for Large Open Spaces Protection 1–14.
- Huang, Y., Wang, E., Bie, Y., 2020. Simulation investigation on the smoke spread process in the large-space building with various height. *Case Stud. Therm. Eng.* 18, 100594. <https://doi.org/10.1016/j.csite.2020.100594>
- Hurley, M.J., Munguia, A., 2007. Analysis of FDS Thermal Detector Response Prediction Capability, NIST GCR 09-921.
- McGrattan, K., Hostikka, S., McDermott, R., Floyd, J., Vanella, M., 2019a. Fire Dynamics Simulator User's Guide. NIST Spec. Publ. 1019 Sixth Ed. 347.
- McGrattan, K., Hostikka, S., McDermott, R., Floyd, J., Weinschenk, C., Overhold, K., 2019b. Fire dynamics simulator (FDS) validation technical reference guide volume 3: Validation. NIST Spec. Publ. 1018 3. <https://doi.org/10.6028/NIST.SP.1018-1>
- McGrattan, K., Hostikka, S., McDermott, R., Floyd, J., Weinschenk, C., Overhold, K., 2013. Fire Dynamics Simulator, Technical Reference Guide, Volume 2: Verification.
- Vianello, C., Mocellin, P., Maschio, G., 2014. Study of formation, sublimation and deposition of dry-ice from carbon capture and storage pipelines. *Chemical Engineering Transactions*, 36, 613-618. <https://10.3303/CET1436103>
- Mocellin, P., Maschio, G., 2016. Numerical modeling of experimental trials involving pressurized release of gaseous CO₂. *Chemical Engineering Transactions*, 53, 349-354. <https://10.3303/CET1653059>
- Mocellin, P., Vianello, C., Maschio, G., 2021. Addressing waste disposal fires in open fields through large eddy simulations. *Chemical Engineering Transactions*, 86, 529-534. <https://10.3303/CET2186089>
- NFPA, 2019. NFPA 72, National Fire Alarm and Signaling Code, National Fire Protection Association.
- NFPA, 2018. FM 3210: Heat detectors for automatic fire alarm signaling.
- Schifiliti, R.P., 2006. , Fire Alarm Systems for Life Safety Code Users, Supplement 2, in: National Fire Protection Association (NFPA). pp. 1113–1138.
- Securiton, 2021. ADW 535 Data Sheet.
- UNI, 2017. UNI/TR 11694:2017, Linea guida per la progettazione, l'installazione, la messa in servizio, la verifica funzionale, l'esercizio e la manutenzione dei sistemi di rivelazione fumo ad aspirazione.
- UNI, 2013. UNI 9795:2013, Stemi fissi automatici di rivelazione e di segnalazione allarme d'incendio - Progettazione, installazione ed esercizio.
- United States Nuclear Regulatory Commission, 2007. Verification and Validation of Selected Fire Models for Nuclear Power Plant Applications. NUREG 1824.
- Vianello, C., Mocellin, P., Maschio, G., Bottacin, G., Dattilo, F., 2020. Waste disposal facilities fires: Prevention and management. the veneto region experience. Paper presented at the Proceedings of the 30th European Safety and Reliability Conference and the 15th Probabilistic Safety Assessment and Management Conference, 3995-4000. doi:10.3850/978-981-14-8593-0_3590-cd
- VVF, 2021. Norme tecniche di prevenzione incendi.